Analog Integrated Circuits and Signal Processing (2018) 94:205–215
https://doi.org/10.1007/s10470-017-1078-0

Enhancement of touch screen sensing based on voltage shifting differential offset compensation

Dong-Min Won[1] · HyungWon Kim[1]

Received: 28 August 2016 / Revised: 21 February 2017 / Accepted: 17 November 2017 / Published online: 4 December 2017

Abstract
In this paper, we present an offset compensation technique to enhance the performance of differential sensing circuits for capacitive touch screens. Accurate offset cancellation of differential circuits is regarded as a difficult problem, especially when the offset changes depending on the input signals. The proposed technique can improve the touch detection SNR by compensating both the input and output offset voltage of the differential integrator. It pre-stores the differential offset voltage and corrects both the positive and negative outputs by shifting them by the ½ of the pre-stored offset voltage. We implemented the proposed technique in a touch screen driving and sensing chip using 65 nm CMOS process. Experiments with three different sensing circuit techniques show that the proposed technique provides an SNR improvement of up to 11.17 dB over conventional sensing circuits.

Keywords Touch screen controller · Integrator · Offset compensation · Voltage shifting

1 Introduction

As projected capacitive touch screen technologies become mature, smartphones, tablet PCs, and notebook computers today increasingly employ capacitive touch screens. Recently, these touch screen technologies have been applied to large screens. However, large touch screens are facing serious detection performance issues: they are highly susceptible to ambient noise. Furthermore, as the panel size increases, the sheet resistance and the self-capacitance of touch sensor films such as indium tin oxide (ITO) films or metal meshes tend to increase. This makes the detection signals (the variation in the mutual capacitance value) suffer from severe attenuation as the signals pass through long paths across the touch screen panel [1–5].

Many previous touch screen detection techniques used single line sensing methods based on single-ended amplifiers. Recently differential sensing methods have been widely adopted, which employ fully differential amplifiers. The differential sensing methods have a strong advantage that it can suppress the common-mode noise of the TSP such as the power supply noise, LCD clock noise, and ambient noise, which are the most prominent noise types. However, differential amplifiers often suffer from an offset of the input and the output bias levels and the device mismatch of the amplifier's differential pair due to process variation [6–9]. Therefore, adding an effective offset compensation technique is essential for the differential sensing methods to provide a desirable performance of noise cancellation.

In this paper, we present a new offset compensation technique for differential sensing methods based on integrators. The proposed offset compensation technique is especially effective in suppressing the offset incurred by process variation, design mismatch, and common mode noise.

✉ HyungWon Kim
hwkim@cbnu.ac.kr

Dong-Min Won
dmwon@cbnu.ac.kr

[1] Department of Electronics Engineering, Chungbuk National University, Cheongju, South Korea

2 Touch screen sensing with differential detection scheme

2.1 Architecture of the differential detection scheme

Figure 1 shows the architecture of differential integrator-based sensing circuit for touch screen controller, which we implemented to compare the performance of the sensing techniques considered in this paper. The differential sensing technique can suppress the common-mode noise from the TSP or the power supply noise, and so it can provide better detection performance than single-line sensing.

The TX driving block of Fig. 1 consists of a DAC, a drive Amp, and TX switches. The DAC retrieves the pre-stored target TX amplitude values from the TX signal memory in digital processing block and converts them to analog signal. The drive Amp amplifies the small voltage swing of the DAC output signal to a TX drive signal of full rail-to-rail swing. The TX block also has inverted non-inverted drive Amps, which produce differential driving TX signals. The differential TX signals allow only the touched effect (mutual capacitance changes) to be passed to the RX lines. This consequently allows the sensing circuit to utilize its maximum dynamic range, and thus leads to a higher SNR.

The driving circuit in Fig. 1 can generate a series of multiple pulses in TX. The differential integrator accumulates the multiple sensing signals, and thus it can further improve the SNR. When the multiple pulse mode is selected, we can configure 2, 4, or 8 pulses for each TX line. The multiple pulses pass through the mutual capacitor in each sensing point of the TSP, and are read out by each RX line.

The sensing signals at each RX line are accumulated by the differential integrator and converted to a static voltage level as a sensing result. In this way, the multiple pulses can suppress the noise and accumulate the sensing signal more effectively, and thus lead to a higher SNR of touch detection [10–13].

2.2 Offset in the differential sensing circuit

While the differential integrator in Fig. 1 provides performance advantages, it can suffer from an offset in its inputs or outputs due to various causes of mismatches. Common sources of such mismatches include the input and the output bias mismatch, and the device mismatch of the differential pair of the operational amplifier (OP Amp), and process variation. The offsets of the differential integrator can substantially degrade the performance. In the following sections, we describe two offset compensation methods used in the proposed differential detection system.

3 Differential integrator with input offset compensation

3.1 Single-rate differential integrator with input offset compensation

Figure 2(a) illustrates a differential integrator with an input offset compensation circuit, and Fig. 2(b) shows the timing diagram of its control signals [14, 15].

During the calibration mode (where CALB is low), the offset compensation circuit samples the unwanted input offset voltage and keeps it in the offset capacitor C_{OFFSET}. In the normal mode, the integrator subtracts the offset

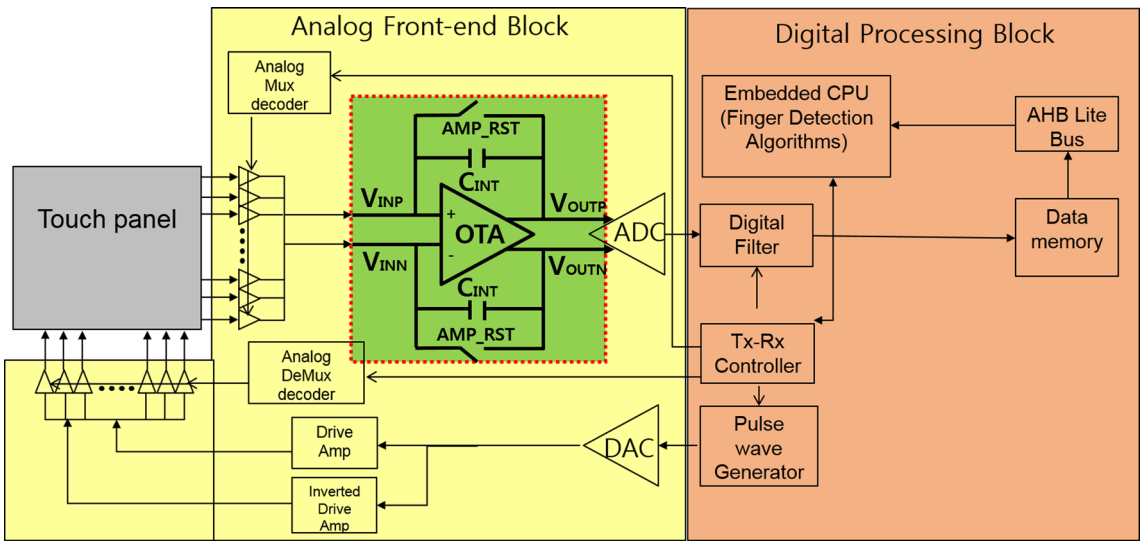

Fig. 1 Architecture of touch screen controller

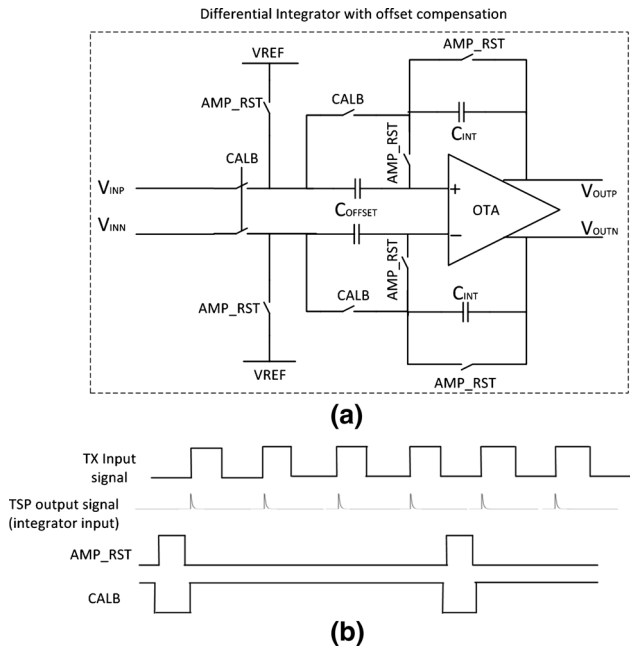

Fig. 2 **a** Timing diagram and **b** architecture of basic differential offset compensation

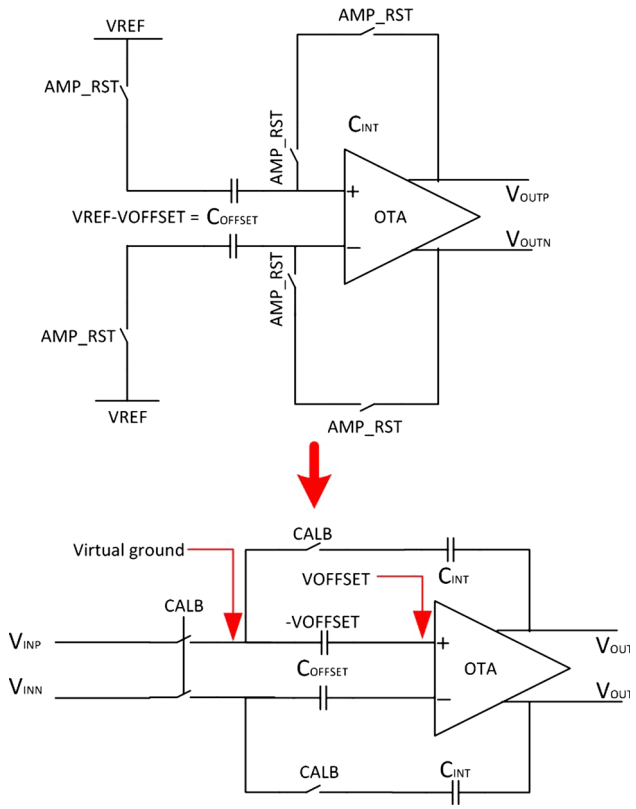

Fig. 3 Description of conventional integrator with differential offset compensation

voltage from the measured sensing signal at the input of the integrator circuit [16, 17].

The operation of input offset compensation circuit of Fig. 2 is illustrated in Fig. 3. When AMP_RST is high, the integrator's feedback capacitor C_{INT} is discharged to 0 V. When CALB is low (or CAL is high), the offset voltage of the OP Amp is captured in the calibration mode. When CALB is high, the integrator operates in the normal mode and integrates the input signal. The two offset capacitors C_{OFFSET}'s store the voltage discrepancies between V_{REF} and the positive and negative inputs of the OP Amp, respectively.

While the differential integrator with the above compensation circuit is effective in compensating the input offset, it is still susceptible to output offsets. The output offsets are often caused by the mismatches in the feedback capacitors, output stage devices in the OP Amp, or the output common-mode voltage levels.

3.2 Double-rate differential integrator with input offset compensation

In this section, a more advanced differential integrator called double-rate differential integrator is described. This integrator can perform twice faster than the single-rate integrator described in the previous section. This section shows that the double-rate differential integrator can use the same input offset compensation circuit as the single-rate circuit.

Figure 4 illustrates the overall sensing circuit employing a double-rate differential integrator with input offset compensation. Its timing diagram is illustrated in Fig. 5, where the positive and negative spike signals from each of the TSP outputs are selected for either the positive or negative input of the differential integrator.

It selects the positive or negative spike signals by using a crossing switches as illustrated in Fig. 4. When RX_PASS is high and RX_CROSS is low, the crossing switches pass the positive spike signals to the integrator. On the other hand, when RX_PASS is low and RX_CROSS is high, the negative spike signals are chosen for integration. When AMP_RST is high, the two feedback capacitors, C_{INT}'s are reset to 0 V. When CAL signal is high, the integrator captures the amplifier's unwanted offset values and stores them in the two offset capacitors C_{OFFSET}'s.

When CALB is high (CAL is low), the integrator converts the sensing signals to step-wise voltage outputs. In the untouched case, the two selected RX lines would have the same amplitude, and so their integration output values are both common-mode voltage, V_{CM} leading to a differential output of 0 V. If one of the two selected RX lines is touched, on the other hand, the signal amplitude of touched RX line would be smaller due to the reduce mutual capacitance. In this case, the differential integrator

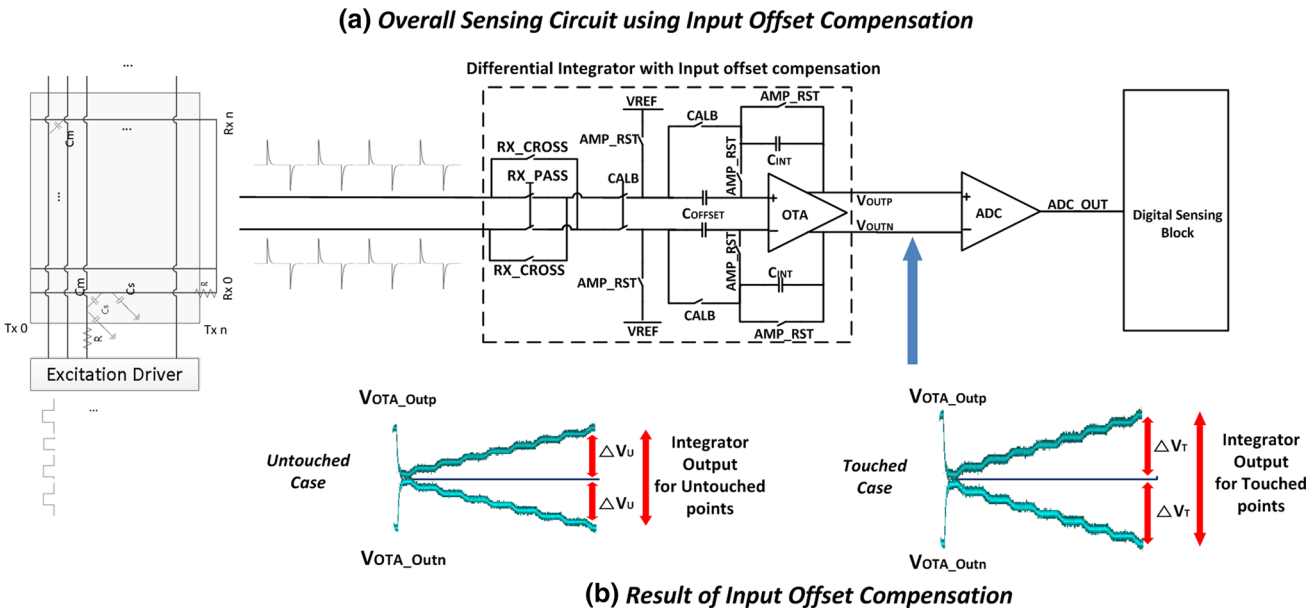

Fig. 4 Architecture of double-rate differential integrator with offset compensation

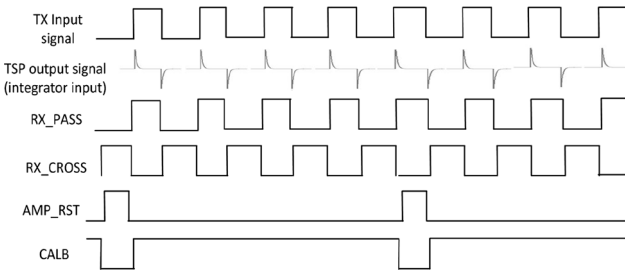

Fig. 5 Timing diagram of double-rate differential integrator with offset compensation

integrates the signal difference between the two RX lines, leading to a large differential output.

Using the way described above, the double-rate differential integrator can achieve double the speed by utilizing both positive and negative RX sensing signals. It also can compensate the input offset in the same way as the single-rate integrator. Just as in the single-rate integrator's offset compensation, however, the output offset of the double-rate integrator can also remain uncompensated. In the following section, we introduce a new technique to compensate the output offset of the differential integrators.

4 Output offset compensation with voltage shifting

As described in Sec. II, the input offset compensation circuit can leave the output offsets uncompensated. Although the ideal differential output of the differential integrator of Fig. 4 is 0 V for the untouched case, various mismatches in an actual sensing circuit incur non-zero differential output, which is defined as the output offset. Such output offset often causes the integration result of touched cases to saturate, when the integrator output with offset exceeds the output dynamic range. Hence the output offset can lead to a reduced Touch Strength, which is defined as the difference between touched and untouched output signals as expressed by Eq. (7). This problem, therefore, tends to degrade the SNR of the sensing results. In this section, we introduce a new offset compensation technique, which removes the input and output offsets of the differential integrator using voltage shifting.

4.1 Structure of voltage shifting offset compensation

Figure 6(a) shows a sensing circuit with the proposed offset compensation. It consists of the following circuit blocks: a differential integrator stage with an input offset compensation, an output offset compensation stage with voltage shifting, an ADC to convert the output offset to digital values, a divide-by-2 operation implemented by a right-shifter by 1-bit, a memory to store the offset values, and a DAC to convert the digital offset values to voltage shift amount. The proposed compensation technique operates in two modes: (1) offset capturing mode and (2) offset shifting mode.

In the offset capturing mode, for every pair of a TX line TX_i and a RX line RX_j, the following operations are repeated: For each sensing point (TX_i, RX_j), no driving signal is applied to produce an untouched output, and the differential output offset value is captured by the output offset

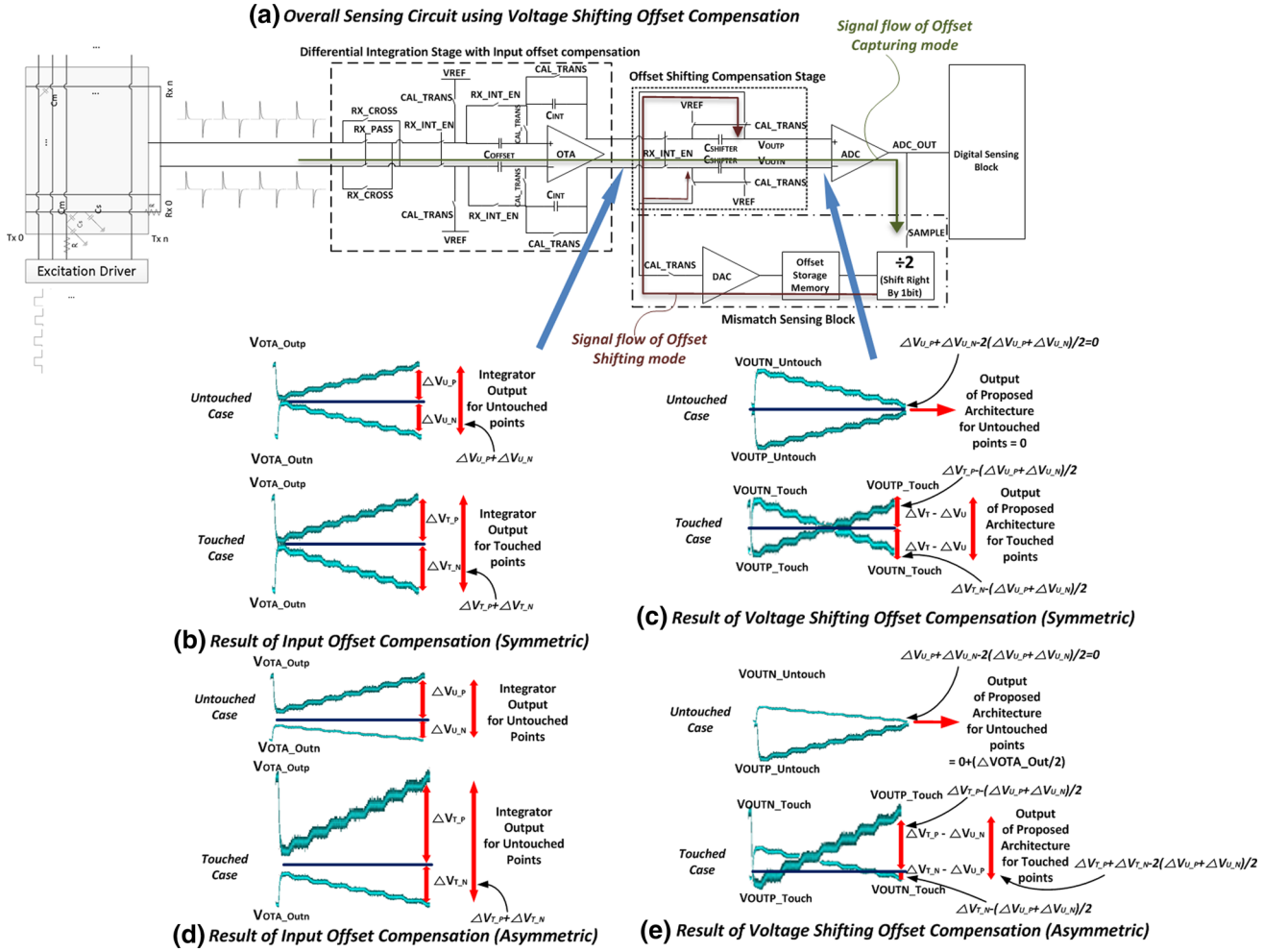

Fig. 6 Architecture of proposed integrator with voltage shifting differential offset compensation

compensation stage. This operation is depicted by the untouched case of Fig. 6(b), where only the input offset compensation is conducted as in the previous section. Here the differential output offset is expressed by $\Delta V_{U\_P} + \Delta V_{U\_N}$.

This output offset is converted to digital data by the ADC, which is divided by 2 using a right-shifting circuit. Then the ½ offset data $(\Delta V_{U_P} + \Delta V_{U_N})/2$ is stored in the offset storage memory at the address corresponding to (TX_i, RX_j). Here only ½ value of the differential offset voltage is stored, since the shifting circuit in Fig. 6(a) pushes the positive and negative outputs by the ½ offset in the opposite direction, respectively, and thus results in a compensation of full offset voltage.

To capture the output offset voltage of all sensing points (TX_i, RX_j), we conduct the offset capturing mode with no TX signals driven during the initialization such as the system power-up or reset process. In Fig. 6(a), the signal flow of the offset capturing mode is highlighted with a green color arrow.

Once the offset capture operation is done for all sensing points, we conduct the offset shifting mode during the normal operation. In the offset shifting mode, for each sensing point (TX_i, RX_j), its pre-stored ½ offset value is read from the offset memory, and converted to an analog voltage by the DAC. Then the output offset compensation stage shifts down the positive output by the ½ offset value, while shifting up the negative output by the ½ offset value. As a result, the final differential output can be accurately corrected to a differential output of 0 V in untouched cases. In Fig. 6(a), the signal flow of the offset shifting mode is highlighted with a brown color arrow.

4.2 Effect of output offset on the touch strength performance

Equations (1)–(9) below describe the performance loss due to the output offset. Using these equations, we explain how the proposed compensation technique can remove the offset.

$$V_{OUTp}^{touch} = \sum_{m=1}^{M}[\int_{0}^{T}(V_{INp} - V_{INn})dt] + V_{OUTp}^{offset} \quad (1)$$

$$V_{OUTn}^{touch} = \sum_{m=1}^{M}\left[\int_{0}^{T}(V_{INn} - V_{INp})dt\right] - V_{OUTn}^{offset} \quad (2)$$

$$V_{OUTdiff}^{touch} = V_{OUTp}^{touch} - V_{OUTn}^{touch} = 2 \times \sum_{m=1}^{M}\left[\int_{0}^{T}(V_{INp} - V_{INn})dt\right] + V_{OUTp}^{offset} + V_{OUTn}^{offset} \quad (3)$$

$$V_{OUTp}^{untouch} = \sum_{m=1}^{M}\left[\int_{0}^{T}(0)dt\right] + V_{OUTp}^{offset} \quad (4)$$

$$V_{OUTn}^{untouch} = \sum_{m=1}^{M}\left[\int_{0}^{T}(0)dt\right] - V_{OUTn}^{offset} \quad (5)$$

$$V_{OUTdiff}^{untouch} = V_{OUTp}^{untouch} - V_{OUTn}^{untouch} = V_{OUTp}^{offset} + V_{OUTn}^{offset} \quad (6)$$

$$TouchStrength = V_{OUTdiff}^{touch} - V_{OUTdiff}^{untouch} = 2 \times \sum_{m=1}^{M}\left[\int_{0}^{T}(V_{INp} - V_{INn})dt\right] \quad (7)$$

$$\left(V_{OUTdiff}^{touch} \leq 2 \times V_{OUT}^{\max}(\text{Required condition})\right) \quad (8)$$

$$TouchStrength \leq 2 \times V_{OUT}^{max} - \left(V_{OUTp}^{offset} + V_{OUTn}^{offset}\right) \quad (9)$$

In Eqs. (1) and (2), V_{INp} and V_{INn} indicate the positive and negative input voltage of the differential integrator, respectively. V_{OUTp}^{touch} represents the positive output of the integrator for a touched input signal, while $V_{OUTp}^{untouch}$ gives the positive output for an untouched input signal. V_{OUTp}^{offset} expresses the offset voltage of the positive output. Similarly, V_{OUTn}^{touch}, $V_{OUTn}^{untouch}$ and V_{OUTn}^{offset} are defined for the negative output. M is the total number of integrations when multiple TX signals are applied to each (TX_i, RX_j) point, while T is the period of one pulse signal to integrate. Equations (3) and (6) express the differential output for the touched and untouched input signals, respectively. Equation (7) defines a performance metric called Touch Strength, expressed by the difference between the touched and untouched differential output. In Eqs. (8) and (9), V_{OUT}^{max} is the maximum dynamic range of the integrator's each output. Equation (8) expresses the restriction imposed on the differential output for touched signals—the restriction that the differential output must be less than $2 \times V_{OUT}^{max}$. Equation (9) gives the upper limit of Touch Strength, which shows that Touch Strength is reduced by the sum of output offset voltage, $V_{OUTp}^{offset} + V_{OUTn}^{offset}$.

To achieve the maximum Touch Strength and thus the best SNR, the proposed method effectively reduces $V_{OUTp}^{offset} + V_{OUTn}^{offset}$. For example, in Fig. 6(b), example input and output signals of the output offset compensation stage are illustrated for differential signals of untouched and touched cases. In this example, we chose $M = 8$. In the untouched case, although the desired differential output is 0 V, the actual differential output of integrator $V_{OUTdiff}^{untouch}$ is non-zero due to the output offset $V_{OUTp}^{offset} + V_{OUTn}^{offset}$. Such non-zero differential output of untouched case restricts the dynamic range of the differential output $V_{OUTdiff}^{touch}$ of touched cases, since the output headroom is reduced by $V_{OUTp}^{offset} + V_{OUTn}^{offset}$. This consequently degrades the SNR performance. On the other hand, the differential output after the output offset compensation stage ensures a zero differential output voltage for all untouched cases, as shown in Fig. 6(c). This maximizes the output headroom to $2 \times V_{OUT}^{max}$, and hence the dynamic range of the touched output to $V_{OUTdiff}^{touch} = 2 \times V_{OUTdiff}^{max}$. Therefore, the proposed compensation technique can provide substantial improvement in the SNR.

4.3 Compensation of symmetric and asymmetric differential offsets

Figure 6(b) and (c) depict an example of compensating the integrator's differential output when the offsets V_{OUTp}^{offset} and V_{OUTn}^{offset} are symmetric in the magnitude. On the other hand, Fig. 6(d) shows an example of the integrator's differential output when asymmetric offsets V_{OUTp}^{offset} and V_{OUTn}^{offset} appear in the outputs. Even in this case, the proposed voltage shifting offset compensation technique can remove the offset. The compensation result of this asymmetric offset is illustrated in Fig. 6(e).

The proposed offset compensation method can cancel both V_{OUTp}^{offset} and V_{OUTn}^{offset} at the same time when the offsets are either symmetric or asymmetric. It first measures the total offset $V_{OUTp}^{offset} + V_{OUTn}^{offset}$ and stores 1/2 of this value to the memory. It calculates the half value $(V_{OUTp}^{offset} + V_{OUTn}^{offset})/2$ by shifting by 1 bit after ADC operation. During the normal operation, the offset shifting compensation stage shifts down V_{OTA}_outp by the half value, while shifting up V_{OTA}_outn by the same half value. It, therefore, can make V_{OTA}_outp and V_{OTA}_outn equal. In the case of symmetric differential offset condition, both V_{OTA}_outp and V_{OTA}_outn become V_{CM} after compensation, and thus provide the maximum possible dynamic range for the ADC, and so the maximum possible SNR. In the case of asymmetric differential offset condition, however, V_{OTA}_outp and V_{OTA}_outn may become a voltage different from V_{CM}, and thus may provide a reduced dynamic range for the ADC. This, however, still can provide considerable increase in the dynamic range for the ADC and so significantly improve the SNR compared with the uncompensated case.

4.4 Operation of offset shifting compensation

Figure 7 illustrates the timing diagram of the proposed voltage shifting compensation circuit. When CAL_TRANS is high, both the input offset and the voltage shifting compensation operations are conducted simultaneously. When RX_INT_EN is high, the integration operations are conducted with multiple TX pulse waves. The integrator's outputs start from the output voltages shifted by the offset values pre-stored, and so the final integration results can provide the maximum Touch Strength. The ADC and DAC used by the output offset compensation stage are not extra circuits. In our touch screen driving and sensing chip, the ADC in the RX sensing circuit is re-used for the offset compensation operation, while the DAC in the TX driving circuit is also re-used. Since our chip contains a large memory to store a few frames of sensing data, the overhead of the offset memory is insignificant. Therefore, the overhead of the proposed offset compensation technique is negligible.

To obtain the best SNR with the proposed output offset compensation technique, we may consider conducting the offset capturing mode repeatedly in every frame's scan. From simulation experiments, however, we found that the output offset voltages for the same (TX_i, RX_j) point stay nearly the same over many frames. Repeating offset capturing mode every frame would also degrade the overall scan rate. In this paper, therefore, we conduct the offset capturing mode only during the power-up initialization and reset cycles.

As a future work, we plan to extend the current work to conduct the offset capturing operation during the offset shifting mode as well. For example, during the offset shifting mode, we can update the memory only for untouched cases, while skipping the touched cases. In this

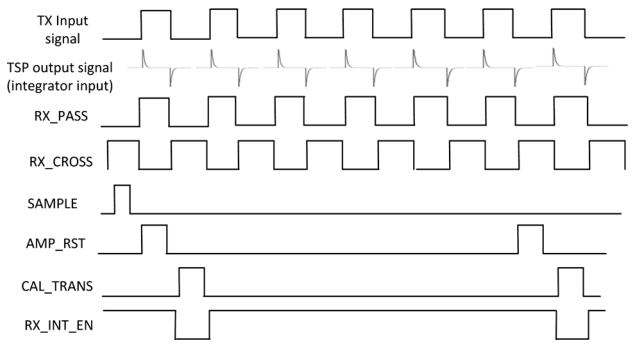

Fig. 7 Timing diagram of proposed integrator with voltage shifting differential offset compensation

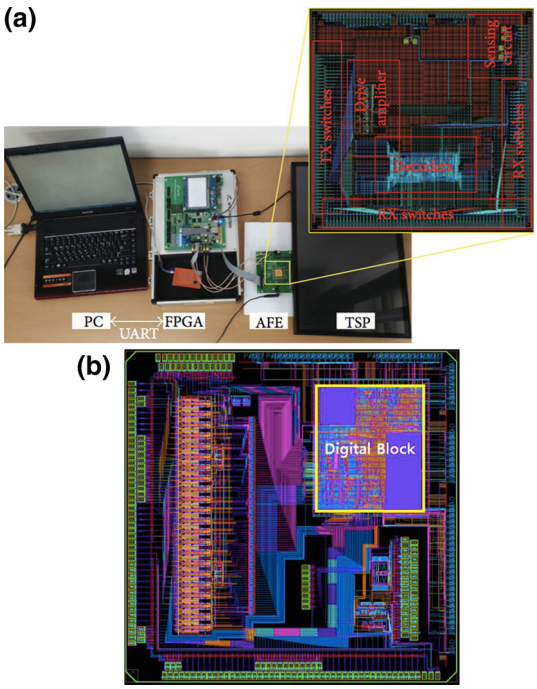

Fig. 9 Implementation of the touch screen controller SoC using the proposed architecture: **a** FPGA and Analog front-end board implementation; **b** 65 nm CMOS ASIC implementation (under fabrication)

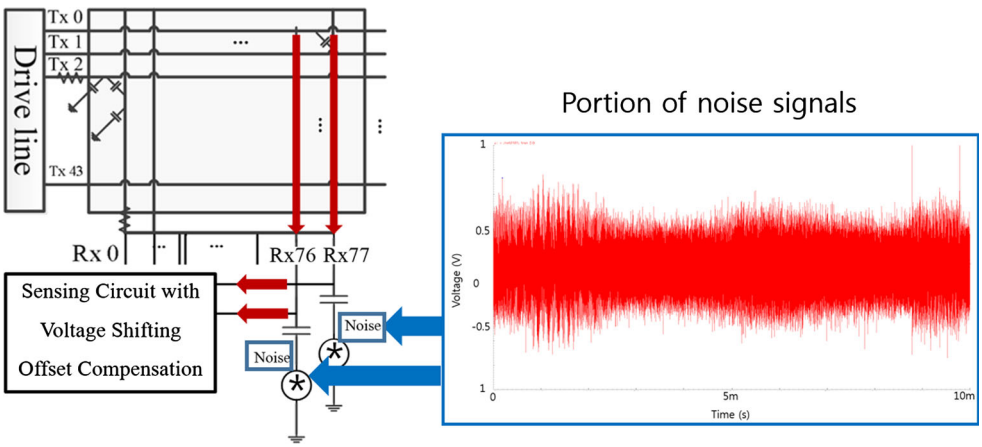

Fig. 8 How to apply portion of noise signals (provided by a world's leading TSP manufacturer)

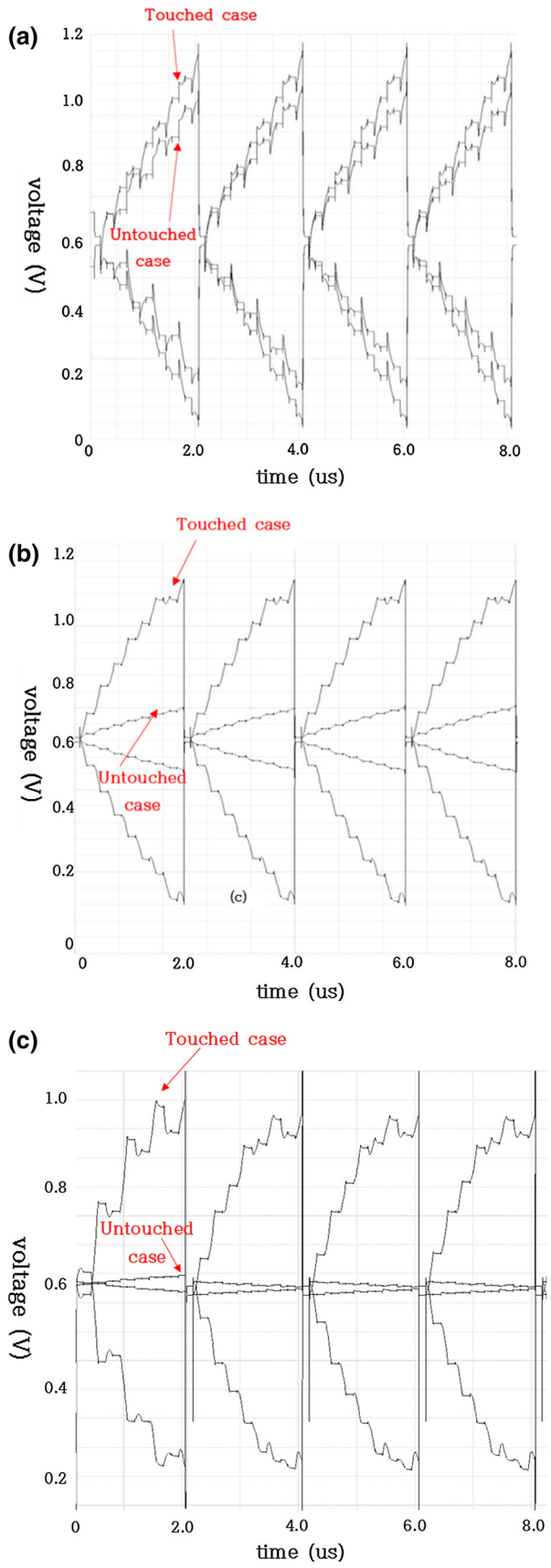

◀**Fig. 10** Comparison simulation result **a** conventional integrator without offset compensation, **b** integrator with input offset compensation, **c** proposed integrator with voltage shifting differential offset compensation

way, most of the offset memory can be updated with new offset values in each frame. This method is expected to make the proposed offset compensation technique more responsive to the fluctuation of offset values due to temperature or supply variation.

5 Experimental results

We designed the differential integrator using the proposed input and output compensation technique. To evaluate its performance, we applied noise signal to an accurate TSP model. Figure 8 illustrates the TSP model and noise signal used in the simulation experiments. It shows a portion of the noise signal, which is realistic noise data provided by the World's leading LCD and touch screen manufacturer [3]. We implemented this sensing circuit as part of a touch screen controller SoC using Samsung 65 nm CMOS process. Figure 9 shows the implementation of the touch screen controller based on the proposed architecture. Figure 9(a) depicts an FPGA implementation with an analog front-end (AFE) board, while Fig. 9(b) shows the final layout of the ASIC implementation using Samsung 65 nm CMOS with 8 metal layers and MIM capacitor. For the ASIC implementation, the die size is 5 × 5 mm, the Vdd is 1.2 V for digital circuit block and 3.3 V for analog RX sensing and TX driving circuit blocks. At the time of writing this article, the ASIC chip is under fabrication, and thus the experimental results in this section is based on simulations with full layout designs and FPGA measurements. We plan to report the measurement results of the chip, once the chip is delivered in the future.

For design and simulation, we used Cadence SPECTRE with an accurate TSP model and measured noise signals. To evaluate the performance of the proposed circuit under realistic conditions, we inserted the measured noise signals to each RX lines. We also injected device size mismatch (10% MOS size mismatch) in the amplifier designs to measure the effectiveness of the proposed offset cancellation. Figure 10(a) shows a simulation result of a conventional differential integrator without offset compensation. Due to the offset of the integrator, its differential output in the untouched case has a large differential swing, and thus leaving very small headroom for the output in the touched case. The Touch Strength (touched signal—the untouched signal) is very small, leading to a large SNR loss. Figure 10(b) shows the result of input offset compensation only. We can observe that the differential output of

Table 1 Performance comparison of three sensing circuits

Sensing Circuit Techniques Experimented	Touch Strength (mV)	SNR gain (dB)
No_Comp: Without offset compensation	Touched: 1.07 V Untouched: 970 mV Touch Strength: 37 mV	47.4 dB = $SNR_{Circuit} - SNR_{TSP}$ = 37.36 dB − (− 10.04 dB)
Input_Comp: With input offset compensation only	Touched: 915 V Untouched: 183 mV Touch Strength: 732 mV	51.1 dB = $SNR_{Circuit} - SNR_{TSP}$ = 41.06 dB − (− 10.04 dB)
Shift_Comp: Proposed input and output offset compensation with voltage shifting	Touched: 827 mV Untouched: 5.96 mV Touch Strength: 821 mV	58.57 dB = $SNR_{Circuit} - SNR_{TSP}$ = 48.53 dB − (− 10.04 dB)

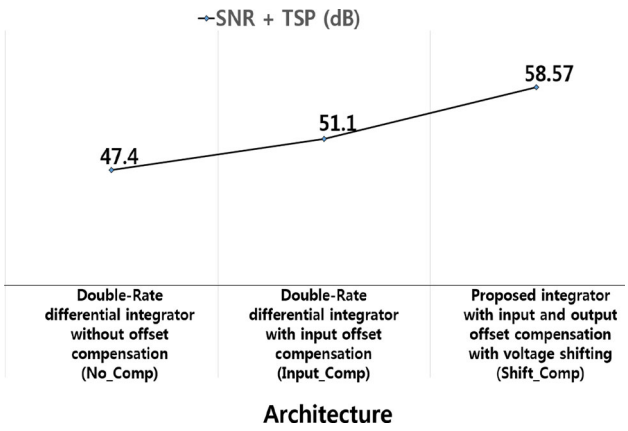

Fig. 11 SNR gain comparison of the three sensing circuits experimented

untouched cases is reduced but still larger than 0 V. Thus it presents an improved Touch Strength, but it is still far from the maximum Touch Strength. Figure 10(c) illustrates the result of the proposed voltage shifting offset compensation. We can observe from Fig. 10(c) that the final integration output in the untouched case is adjusted to the desired value, 0 V. In Fig. 10(c), the output of touched cases, therefore, can have the maximum dynamic range of the integrator. This ensures to achieve the maximum Touch Strength like the ideal integrator with no offset.

Using the equations below, we describe how to calculate the Touch Strength, and Signal to Noise Ratio (SNR) of touch screen sensing circuits.

$$TouchStrength = Signal_{Avg}^{Touched} - Signal_{Avg}^{Untouched} \quad (10)$$

$$Noise_{RMS}^{Touched} = \sqrt{\frac{\Sigma_{N_{Samples}}\left(Signal[n] - Signal_{Avg}^{Touched}\right)}{N_{Samples}}} \quad (11)$$

$$SNR(dB) = 20Log\frac{TouchStrength}{Noise_{Avg}^{Touched}} \quad (12)$$

$$SNRGain(dB) = (SNR\ of\ Sensing\ Circuit\ Output) - (SNR\ of\ TSP\ RX\ Output) \quad (13)$$

Equation (10) expresses Touch Strength, which is defined by the difference of average signal (voltage) between the touched and untouched cases. Then Eqs. (11)–(13) express the Noise RMS (root mean square) value, SNR, and SNR gain respectively. The SNR calculation given by Eqs. (10)–(12) is a common method widely used by the touch screen industry and research community [13]. In order to make fair comparison among various sensing techniques under different conditions such as different TSP, driving signals, and noise signals, we use SNR gain instead of SNR. The SNR gain of Eq. (13) is a relative SNR enhancement obtained by the sensing circuit over the reference SNR of TSP's RX output. Thus the SNR gain gives a constant value regardless of the changes in the driving signals, noise signals, and the TSP's properties, while the SNR varies along with such changes.

To evaluate the performance improvement of the proposed technique, we have implemented the following three different sensing techniques using 65 nm CMOS technology:

(1) Double-rate differential integrator without offset compensation (No_Comp).

Table 2 Performance comparison with previous works

Offset Compensation Architectures	SNR gain (dB)
Proposed architecture	58.57 dB = $SNR_{Circuit} - SNR_{TSP}$ = 48.53 dB − (− 10.04 dB)
[5]	43.9 dB = $SNR_{Circuit} - SNR_{TSP}$ = 15.52 dB − (− 27.86 dB)
[6]	56.88 dB = $SNR_{Circuit} - SNR_{TSP}$ = 46.84 dB − (− 10.04 dB)

(2) Double-rate differential integrator with only input offset compensation (Input_Comp).
(3) Double-rate differential integrator with both input and output offset compensation using voltage shifting (Shift_Comp).

Table 1 compares the differential outputs of touched and untouched cases for these three sensing techniques. In the 2nd column of Table 1, Shift_Comp provides the largest Touch Strength. Input_Comp shows the next largest, while No_Comp gives the smallest Touch Strength.

The 3rd column in Table 1 shows the SNR gain values of the three sensing techniques, which are also illustrated in Fig. 11. Here the SNR gain was obtained by subtracting the SNR of the TSP output from the SNR of the sensing circuit output as expressed by Eq. (13).

We conducted the simulation experiments and measured the performance using an accurate model of a 23-in commercial touch screen panel and the noise signals described in Fig. 8. Shift_Comp provides an SNR gain of 58.57 dB, which is 11.17 and 7.47 dB higher than No_Comp and Input_Comp, respectively. This is regarded as substantial performance improvement at a reasonable cost of circuit complexity.

Table 2 compares the SNR gain of the proposed architecture with previous work. [5] reports a method of increasing the touch strength by reversing the touched and untouched outputs of the integrator followed by differential amplifier. It reverses the touched and untouched outputs by adding a fixed voltage to a single-ended integrator output, which in effect shifts the output voltages in the opposite direction. The differential amplifier boosts the output voltage and so further increases the touch strength, which in turn increases the SNR. This method, however, has a limited SNR improvement, because it has only single-ended integrator and a fixed amount voltage shifting for all TX and RX lines. [6] presents a rotating auto-zeroing offset cancellation architecture, which is effective in touch screens with continuous driving signals with a readout circuit based on a differential voltage amplifier.

In contrast, our proposed method employs a fully differential integrator and also allows different amount of voltage shifting for each pair of TX and RX lines. From extensive measurements with various commercial touch screen panels, we have observed that different pairs of TX and RX lines often induce varying offset voltages at the integrator outputs due to different signal propagation property depending on the paths across the touch screen panel. Such varying offset voltages require customized compensating method for each pair of TX and RX lines. The key advantage of the proposed architecture is the customized offset compensation of every pair of TX and RX lines using its own offset measurement pre-stored in memory. In Table 2, the SNR gain reported by [5] and [6] are 43.9 and 56.88 dB, respectively, while the proposed architecture achieves a higher SNR gain of 58.57 dB.

6 Conclusions

We proposed an efficient offset compensation technique that can substantially improve the SNR of differential sensing circuits for touch screens. The proposed voltage shifting differential offset compensation technique can effectively eliminate both the input and output offset voltages of differential integrators. It suppresses the input offset by employing differential structure of offset capacitors. It captures and stores the output offset, and then eliminates the output offset by shifting the integrator output by the pre-stored offset values. We have shown that the propose technique can effectively compensate the sensing circuit's differential offset whether the offset is symmetric or asymmetric using only one offset storage memory.

Experimental results show that the proposed technique provides an SNR improvement of 11.17 dB over the non-compensated sensing circuit, and 7.47 dB over the sensing technique with only input offset compensation. Since it can reuse the existing ADC and DAC, its area overhead is relatively small. Therefore, the proposed technique is an effective approach to a significant performance enhancement with low circuit complexity for high performance touch screen sensing.

Acknowledgements This research was supported by IITP grant funded by the Korean government (No. R7117-19- 0164, Development of wide area driving environment awareness and cooperative driving technology which are based on V2X wireless communication).

References

1. Mohamed, M. G. A., Kim, H. W., & Cho, T. W. (2014). Efficient multi-touch detection algorithm for large touch screen panels. *IEIE Transactions on Smart Processing and Computing, 3*(4), 246–250.
2. Lee, J., Yeo, D.-H., Um, J.-Y., Song, E.-W., Sim, J.-Y., Park, H.-J., Seo, S.-M., Shin, M.-H., Cha, D.-H., Lee, H. (2012). A 10-touch capacitive-touch sensor circuit with the time-domain input-node isolation. In *SID 2012 DIGEST* (Vol. 43, Issue 1, pp. 493–496).
3. Mohamed, M. G. A., & Kim, H. (2015). Concurrent driving method with fast scan rate for large mutual capacitance touch screens. *Journal of Sensors*, *2015*, no. 768293.
4. Choi, G., Mohamed, M. G. A., & Kim, H. (2014). Distributed architecture of touch screen controller SoC for large touch screen panels. In *IEEE international SoC design conference* (pp. 22–23).
5. Seo, I., Jang, U., Mohamed, M., et al. (2014). Voltage shifting double integration circuit for high sensing resolution of large capacitive touch screen panels. In *IEEE international symposium on consumer electronics*.

6. Won, D.-M., & Kim, H. (2015). Touch screen sensing circuit with rotating auto-zeroing offset cancellation. *Journal of Information and Communication Convergence Engineering, 13*(3), 189–196.
7. Kim, J., Mohamed, M. G. A., Kim, H. (2015). Design of a frequency division concurrent sine wave generator for an efficient touch screen controller SoC. In *IEEE international symposium on consumer electronics (ISCE)*.
8. Ragheb, A., Kim, H. (2016). Differentiator based sensing circuit for efficient noise suppression of projected mutual-capacitance touch screens. In *International conference on electronics, information, and communication*.
9. Choi, G.-S., & Kim, H. (2016). New FFT design with enhanced scan rate for frequency division concurrent sensing of mutual-capacitance touch screens. In: *International conference on electronics, information, and communication*.
10. Seo, I., Cho, T., Kim, H., Jang, H.-G., & Lee, S.-W. (2013). Frequency domain concurrent sensing technique for large touch screen panels. In *Proceedings of the IEEK conference, 2013* (pp. 55–58).
11. Mohamed, M. G. A., Jang, U.Y., Seo, I.C., Kim, H., Cho, T.-W., Jang, H.-G., & Lee, S.-W. (2014). Efficient algorithm for accurate touch detection of large touch screen panels. In *Proceedings of International Symposium on Consumer Electronics* (pp. 243–244).
12. Jang, U. Y., Kim, H. W., & Cho, T. W. (2015). Frequency division concurrent sensing method for high-speed detection of large touch screens. *Journal of the Korea Institute of Information and Communication Engineering (JKIICE), 19*(4), 895–902.
13. Seo, I. C., & Kim, H. W. (2015). Dual sensing with voltage shifting scheme for high sensitivity touch screen detection. *Journal of the Institute of Electronics and Information Engineers, 52*(4), 71–79.
14. Kugelstadt, T. (2005). Auto-zero amplifiers ease the design of high-precision circuits. Texas Instruments Incorporated.
15. Kwon, Young-Cheon, & Kwon, Oh-Kyong. (2013). A precision mismatch measurement technique for integrated capacitor array using a switched capacitor amplifier. *IEEE Transactions on Semiconductor Manufacturing, 26,* 226–232.
16. Enz, C. C., & Temes, G. C. (1996). Circuit techniques for reducing the effects of op-amp imperfections: Autozeriong, correlated double sampling, and chopper stabilization. *Proceedings of IEEE, 84*(11), 1584–1614.
17. ATMEL Corporation. (2004). Touch Sensors Design Guide, 10620D-AT42.

DongMin Won received his B.S., and M.S. degrees in Electronics Engineering from Chungbuk National University, Cheongju, South Korea in 2014 and 2016, respectively. He is currently with SiliconWork Inc. working as a analog and mixed signal chip design engineer. His current research interest includes mixed signal IC design, analog circuit design, SoC design, Display IC designs, Touch Screen Sensing Circuit design.

HyungWon Kim received his B. S. and M. S. degree in Electrical Engineering from Korea Advanced Institute of Science and Technology (KAIST) in 1991 and 1993, respectively, and Ph. D. degree in Electrical Engineering and Computer Science from the University of Michigan, Ann Arbor, MI, US in 1999. In 1999, he joined Synopsys Inc., Mountain View, CA, US, where he developed electronic design automation software. In 2001, he joined Broadcom Corp., San Jose, CA, US, where he developed various network chips including a WiFi gateway router chip, a network processor for 3G, and 10gigabit ethernet chips. In 2005, he founded Xronet Corp., a Korea based wireless chip maker, where as a CTO and CEO, he managed the company to successfully develop and commercialize wireless baseband and RF chips and software including WiMAX chips supporting IEEE802.16e and WiFi chips supporting IEEE802.11a/b/g/n. Since 2013, he has been with Chungbuk National University, Cheongju, South Korea, where he is an associate professor in the department of Electronics Engineering. His current research focus covers the areas of sensor read-out circuits, touch screen controller SoC, wireless sensor networks, wireless vehicular communications, mixed signal SoC designs for low power sensors, and bio-medical sensors.